

## Brain endothelial dysfunction in cerebral adrenoleukodystrophy

Patricia L. Musolino,<sup>1,2,\*</sup> Yi Gong,<sup>1,2,\*</sup> Juliet M. T. Snyder,<sup>1</sup> Sandra Jimenez,<sup>1</sup> Josephine Lok,<sup>3</sup> Eng H. Lo,<sup>3</sup> Ann B. Moser,<sup>4</sup> Eric F. Grabowski,<sup>5</sup> Matthew P. Frosch<sup>1,6</sup> and Florian S. Eichler<sup>1,2</sup>

\*These authors contributed equally to this work.

See Aubourg (doi:10.1093/awvxxx) for a scientific commentary on this article.

X-linked adrenoleukodystrophy is caused by mutations in the *ABCD1* gene leading to accumulation of very long chain fatty acids. Its most severe neurological manifestation is cerebral adrenoleukodystrophy. Here we demonstrate that progressive inflammatory demyelination in cerebral adrenoleukodystrophy coincides with blood–brain barrier dysfunction, increased MMP9 expression, and changes in endothelial tight junction proteins as well as adhesion molecules. *ABCD1*, but not its closest homologue *ABCD2*, is highly expressed in human brain microvascular endothelial cells, far exceeding its expression in the systemic vasculature. Silencing of *ABCD1* in human brain microvascular endothelial cells causes accumulation of very long chain fatty acids, but much later than the immediate upregulation of adhesion molecules and decrease in tight junction proteins. This results in greater adhesion and transmigration of monocytes across the endothelium. PCR-array screening of human brain microvascular endothelial cells after *ABCD1* silencing revealed downregulation of both mRNA and protein levels of the transcription factor c-MYC (encoded by *MYC*). Interestingly, *MYC* silencing mimicked the effects of *ABCD1* silencing on *CLDN5* and *ICAM1* without decreasing the levels of *ABCD1* protein itself. Together, these data demonstrate that *ABCD1* deficiency induces significant alterations in brain endothelium via c-MYC and may thereby contribute to the increased trafficking of leucocytes across the blood–brain barrier as seen in cerebral adrenoleukodystrophy.

1 Department of Neurology, Massachusetts General Hospital, Boston, MA, USA

2 Center for Rare Neurological Diseases, Massachusetts General Hospital, Boston, MA, USA

3 Neuroprotection Research Laboratory, Departments of Radiology and Neurology, Massachusetts General Hospital, Charlestown, MA, USA

4 Hugo W Moser Research Institute, Kennedy Krieger Institute, Baltimore, MD, USA

5 Department of Paediatric Haematology/Oncology, Massachusetts General Hospital, Boston, MA, USA

6 C.S. Kubik Laboratory for Neuropathology, Massachusetts General Hospital, Boston, MA, USA

Correspondence to: Dr Florian S. Eichler,  
Massachusetts General Hospital,  
Department of Neurology,  
55 Fruit Street,  
WAC 708, MA 02114,  
USA  
E-mail: feichler@partners.org.

**Keywords:** genetics; neurodegeneration; demyelination; leukodystrophy; neuroinflammation; blood–brain barrier

**Abbreviations:** (C)ALD=(cerebral) adrenoleukodystrophy; HBMEC=human brain microvascular endothelial cell; HUVEC = human umbilical vein endothelial cell; VLCFA = very long-chain fatty acid

Received April 5, 2015. Revised June 19, 2015. Accepted July 3, 2015.

© The Author (2015). Published by Oxford University Press on behalf of the Guarantors of Brain. All rights reserved. For Permissions, please email: journals.permissions@oup.com

## Introduction

X-linked adrenoleukodystrophy (ALD) is a devastating disorder caused by mutations in the *ABCD1* gene and characterized by the accumulation of very long-chain fatty acids (VLCFAs) in plasma and affected tissues (Mosser *et al.*, 1993; Moser *et al.*, 2004). The *ABCD1* gene encodes the peroxisomal ABC half-transporter ABCD1 (formerly adrenoleukodystrophy protein, ALDP). The ATP-binding domain of ABCD1 faces the cytosol and substrates, such as C26:0-CoA, C24:0-CoA, and C22:0-CoA, are transported from the cytosol into the peroxisome, allowing for degradation of these fatty acids by peroxisomal  $\beta$ -oxidation.

Forty per cent of male children and up to 40% of adult patients (Eichler *et al.*, 2007) with ALD will convert to a rapidly progressive form of inflammatory demyelination (cerebral ALD; CALD) that leads to progressive neurological decline, vegetative state and death within 2–3 years. It is clear that other factors ('hits') modulate this phenotypic conversion, as the *ABCD1* mutation is necessary but not sufficient to develop cerebral disease. Blood–brain barrier disruption with migration of leucocytes to the brain, as indicated by a rim of contrast enhancement on MRI (Melhem *et al.*, 2000) and the presence of marked perivascular inflammatory cells on histopathology (van der Voorn *et al.*, 2011), has for a long time been implicated as crucial to this conversion.

Neuroimaging studies are exquisitely sensitive in detecting the initial plaque of the expanding confluent lesion (Moser *et al.*, 2000; Loes *et al.*, 2003). Use of gadolinium-diethylenetriamine penta-acetic acid (Gd-DPTA) demonstrates a fringe of accumulated contrast material behind the leading edge of the lesion (Melhem *et al.*, 2000). This contrast enhancement appears to correspond to the histologically mapped zone of active inflammation (van der Voorn *et al.*, 2011). Decreased white matter perfusion has also been found beyond this advancing inflammatory edge (Musolino *et al.*, 2012). Together with contrast enhancement, this appears to predict lesion progression (Melhem *et al.*, 2000), suggesting a role of blood–brain barrier disruption in the pathophysiology of ALD. Moreover, there are several reports that a moderate or severe head trauma can initiate the conversion to rapidly progressive inflammatory demyelination at the site of the original contusion (Weller *et al.*, 1992; Berger *et al.*, 2010; Raymond *et al.*, 2010). This again emphasizes the importance of blood–brain barrier integrity in ALD.

Despite extensive research in other common inflammatory demyelinating diseases such as multiple sclerosis and acute demyelinating encephalomyelopathy (ADEM), the mechanisms by which the blood–brain barrier changes its permeability to circulating leucocytes remain unknown (Law *et al.*, 2004; Wuerfel *et al.*, 2004; Goverman, 2009). In this regard CALD, where a single gene defect predisposes to brain inflammation, provides a unique

opportunity to elucidate the genetic, molecular and cellular bases of pathologic blood–brain barrier permeability. The blood–brain barrier is formed by specialized endothelial cells, pericytes and astrocytes, and regulates the interaction between the immune and nervous systems (Obermeier *et al.*, 2013). Leucocyte infiltration is considered a critical step in the pathogenesis of many CNS diseases (Weckerle *et al.*, 1986; Cross *et al.*, 1990; Raine *et al.*, 1990; Zlokovic, 2008), but in normal brain leucocyte traffic into the CNS is limited in part because brain endothelium is much tighter than elsewhere in the body (Man *et al.*, 2008; Zlokovic, 2008; Wilson *et al.*, 2010).

It is well accepted that activation of brain endothelium by inflammation increases the expression of MMP9 and adhesion molecules and causes tight junctions to open, promoting translocation of circulating leucocytes into the brain (Harkness *et al.*, 2000). To date there have been no studies of brain endothelium in CALD. The purpose of this study is to provide a first assessment of the effects of ABCD1 deficiency upon brain endothelium and its role in the pathogenesis of CALD. We examined brain endothelial markers involved in endothelial–leucocyte interactions and blood–brain barrier permeability in CALD brain autopsy specimens using immunohistochemistry and immunofluorescence and found profound changes. To determine whether these changes are secondary to surrounding inflammation or the direct effect of dysfunctional ABCD1 in brain endothelium, we studied *in vitro* systems of human brain microvascular endothelial cells.

## Materials and methods

### Human central nervous system specimens

This study was performed on post-mortem brain tissue from 21 ALD ( $n = 13$  CALD,  $n = 4$  adrenomyeloneuropathy,  $n = 4$  female heterozygotes), six relapsing remitting multiple sclerosis ( $n = 6$ ), and 11 control cases obtained from the Brain and Tissue Bank for Developmental Disorders at the University of Maryland in Baltimore. Use of this material was approved by the Institutional Review Board of Massachusetts General Hospital. Patient characteristics and conditions are listed in Table 1. All samples analysed from patients with CALD had advanced lesions involving portions of the subcortical white matter, but sparing U-fibres. Control tissue from these banks consisted of patients who died without neurological disorders. All ALD samples were biochemically confirmed.

### Immunofluorescence and histochemical staining

For human brain immunofluorescence staining, frozen unfixed brain tissue from ALD, multiple sclerosis and control autopsies were fixed using 4% paraformaldehyde for 2 h, cryopreserved on 20% sucrose for 48 h, and then frozen and cut with a cryostat (Microm, Zeiss) at 16- $\mu$ m section thickness, at

**Table 1 Patient autopsy sample characteristics**

UMN#	Phenotype	Age (years)	Gender	PMI (h)
582	CCALD	6	Male	12
1591	CCALD	8	Male	1
340	CCALD	9	Male	9
595	CCALD	10	Male	1
843	CCALD	13	Male	2
578	CCALD	13	Male	14
612	CCALD	17	Male	5
1723	CCALD	23	Male	16
1691	CCALD	28	Male	10
1098	CCALD	28	Male	18
1122	ACALD	33	Male	6
861	ACALD	39	Male	7
188	ACALD + AMN	39	Male	5
864	AMN	35	Male	40
5433	AMN	58	Male	17
5001	AMN	63	Male	23
4692	AMN	77	Female	18
787	ALD, X-linked, carrier	77	Female	12
1145	ALD, X-linked, carrier	78	Female	22
998	ALD, X-linked, carrier	81	Female	27
4691	ALD, X-linked, carrier	88	Female	10
330	MS	42	Female	37
711	MS	45	Female	18
1491	MS	55	Male	3
1709	MS	57	Female	3
5466	MS	55	Female	5
1593	MS	65	Female	2
4898	Control	7	Male	12
4337	Control	8	Male	16
1860	Control	8	Male	5
5391	Control	8	Male	3
1674	Control	8	Male	36
1376	Control	37	Male	12
1134	Control	41	Male	15
5404	Control	50	Male	17
5568	Control	52	Male	17
5237	Control	52	Male	13
5088	Control	66	Male	23

AMN = adrenomyeloneuropathy; UMN# = University of Maryland Brain Bank Number; PMI = post-mortem interval to brain harvesting; MS = multiple sclerosis. Selected adrenomyeloneuropathy specimens did not have inflammatory demyelinating lesions (CALD).

–23°C. Each tissue section was mounted on a glass slide, allowed to dry, rinsed twice in phosphate-buffered saline, and dehydrated. All sections were then incubated overnight in a humid chamber at 4°C with primary antibodies (Supplementary Table 1) diluted in phosphate-buffered saline containing 0.2% (w/v) bovine serum albumin and 0.03% Triton™ X-100. After rinsing in phosphate-buffered saline, sections were incubated for 1 h at 37°C with their respective species-specific secondary antibodies conjugated to FITC, Cy-3 (Jackson Immuno Research Inc.), or Alexa Fluor® 467 and mounted with ProLong® Gold Antifade mountant with DAPI (Life Technologies).

Immunohistochemistry was performed on formalin-fixed, paraffin-embedded 5 µm sections. An indirect

immunohistochemical technique using the streptavidin-biotin system was conducted, using diaminobenzidine as a chromogen. Sections were incubated overnight at 4°C with primary antibodies (Supplementary Table 1). Slides were then rinsed twice in phosphate-buffered saline and incubated at room temperature for 1 h with biotinylated secondary antibodies (1:200, Vector Labs), rinsed twice in phosphate-buffered saline, and incubated with ABC (Vectastain Elite kit, Vector Labs) for 1 h at room temperature. Peroxidase activity was demonstrated by reaction with 3,3'-diaminobenzidine using H<sub>2</sub>O<sub>2</sub> and nickel salts for enhancement of the reaction product. After dehydration, the sections were coverslipped with synthetic Canada balsam as mounting media.

For endothelial cell immunofluorescence, human brain microvascular endothelial cells (HBMECs) and human umbilical vein endothelial cells (HUVECs) were cultured in 8-well slide chambers and silenced with *ABCD1* for 48 h. Cells were then fixed with 4% paraformaldehyde for 10 min and permeabilized in blocking buffer containing 0.3% Triton™ X-100 and 2% goat serum for 1 h. Cells were then stained with CLDN5 and ICAM1 primary antibodies at 4°C overnight, followed by incubation with Alexa Fluor® 488 or 555 conjugated secondary antibodies, and then mounted in mounting medium with DAPI (Vector Lab).

## Confocal microscopy and image analysis

Sections were imaged using 80i Eclipse Nikon fluorescence and Zeiss confocal microscopes. In human autopsy specimens, we quantified the expression of different antibodies in three different zones (cortex, perilesional white matter and core) of the demyelinating lesion. Five consecutive photographs at ×20 magnification were taken in each zone, and the total area of fluorescence was quantified using ImageJ software. The average of the area for each specimen was used for comparisons.

## Cell cultures

Primary HBMECs from CSC systems were a generous gift from Drs Eng Lo and Josephine Lok at Massachusetts General Hospital. They were maintained in endothelial cell basal medium (EBM-2) containing EGM-MV SingleQuots kit (Lonza) onto collagen-coated 25 cm<sup>2</sup> flasks in a 37°C humidified atmosphere of 95% air and 5% CO<sub>2</sub>. In collaboration with Dr. Grabowski's laboratory, primary HUVECs were obtained from freshly isolated umbilical cords post-parturition (as approved by the Institutional Review Board of Massachusetts General Hospital) by treatment with collagenase (280 U/ml) for 10 min and collected in a 50 ml falcon tube. After being centrifuged at 1250 rpm for 5 min, the cell pellet was dissolved in 10 ml endothelial cell medium containing M199 (Gibco®) with NaHCO<sub>3</sub> (2.2 mg/ml), HEPES (5.9 mg/ml) (Lonza), and 10% human serum, and penicillin-streptomycin-glutamine, before being cultured in T75 flasks. After 2 days, cells were plated in 24-well culture plates coated with collagen and maintained in endothelial cell medium supplemented with 10% foetal bovine serum, 2 mM L-glutamine, 50 µg/ml heparin, and 50 µg/ml endothelial growth factors (Biomedical Technologies Inc.) at 37°C in a humidified atmosphere containing 5% CO<sub>2</sub> until they reached confluence.

## ABCD1 and MYC gene silencing

*ABCD1* and *MYC* (also known as *c-MYC*) in primary HBMEC were silenced via siRNA (DharmaFECT<sup>®</sup>, GE healthcare) with non-targeting siRNA treatment as control and incubated for 48 and 72 h according to the protocol provided by the manufacturer. Briefly,  $1.5\text{--}2 \times 10^5$  HBMEC and HUVEC cells were seeded in 6-well plates for 24 h. siRNA dissolved in serum free-medium was mixed with DharmaFECT<sup>®</sup> transfection reagent and incubated for 20 min at room temperature. Cells were then replaced with fresh medium containing 25 nM either non-targeting or siRNA, targeting either *ABCD1* or *MYC*, and then cultured for specific time periods for further analysis.

## Quantitative real time reverse transcription-polymerase chain reaction

Total RNA was isolated by using Qiagen RNeasy<sup>®</sup> Mini Kit (Qiagen). First-strand cDNA synthesis used 100 ng random primer (Life Technologies), 1.0  $\mu\text{g}$  total RNA, 10 mM dNTP, and 200 units of reverse transcriptase (Life Technologies) per 20  $\mu\text{l}$  reaction. PCRs were performed in duplicates in a 25  $\mu\text{l}$  final volume by using SYBR Green<sup>®</sup> master mix from Applied Biosystems (Life Technologies), and the data were analysed by calculating the  $\Delta\text{Ct}$  value between testing gene and internal control. Primers used in the experiment were as described in Supplementary Table 2. For the human multiple sclerosis RT<sup>2</sup> profiler<sup>™</sup> PCR array, cells were treated with either non-targeting or *ABCD1* siRNA and collected for RNA extraction using Qiagen RNeasy<sup>®</sup> Mini Kit (Qiagen). First strand cDNA were synthesized using RT<sup>2</sup> First strand kit (Qiagen) and SYBR Green<sup>®</sup> PCR array was performed according to the manufacturer's instructions.

## Polymerase chain reaction array

We profiled gene expression in HBMECs after *ABCD1* silencing using The Human Multiple Sclerosis RT<sup>2</sup> Profiler<sup>™</sup> PCR Array (Qiagen), which contains 84 key genes related to auto-inflammation in the CNS, including cytokine/chemokine receptors, cell adhesion, apoptosis, and cell stress (Supplementary Table 3). Briefly, cells were treated with either non-targeting or *ABCD1* siRNA and collected for RNA extraction using Qiagen RNeasy<sup>®</sup> Mini Kit (Qiagen). First strand cDNA were synthesized using RT<sup>2</sup> First strand kit (Qiagen) and SYBR PCR array was performed according to the manufacturer's instructions.

## Western blot protein analysis

Tissue and cell lysates were prepared by using RIPA buffer (Sigma-Aldrich) with 1% Halt Protease and Phosphatase Inhibitor Cocktail (Roche). Protein samples were separated on NuPAGE<sup>®</sup> 4–12% Bis-tris gels (Life Technologies) and transferred on PVDF membranes. Membranes were blocked with 5% non-fat milk in phosphate-buffered saline containing 0.05% Tween 20 and probed with antibody against different kinds of antibodies diluted in blocking buffer including human *ABCD1* and *ABCD2* (Origene) and *ZO1* (encoded by *TJP1*)

(Life Technologies), PECAM and VCAM1 (Santa Cruz), ICAM1 (Sino Biological Inc.), *c-MYC*, *CLDN5*, and *ABCD3* (Abcam). Anti- $\beta$ -actin (Santa Cruz) was used as a protein loading control. Membranes were developed with SuperSignal<sup>®</sup> West Pico Chemiluminescent Substrate (Thermo Scientific) after incubation with horseradish peroxidase-conjugated secondary antibodies.

## Lipid analysis

Lipid analysis was performed on cell pellets at 48, 72 and 96 h after silencing. The samples were dried, weighed, and extracted with methanol. The lysophosphatidylcholines were analysed by combined liquid chromatography-tandem mass spectrometry following methods previously described (Hubbard *et al.*, 2009). Absolute values of C26:0 lysophosphatidylcholine were reported.

## Very long-chain fatty acid treatment

HBMECs were seeded at a density of  $1.5 \times 10^5$  cells per well in a 6-well plate and incubated at 37°C for 24 h. Cells (untreated, non-targeting, and *ABCD1* siRNA) were treated with VLCFA (C26:0 lysophosphatidylcholine, 30  $\mu\text{M}$ ) added to the culture media for 48 h before collection for western blot.

## Human monocyte-endothelial adhesion assay

In the adhesion assay, the three conditions of HBMEC (untreated, non-targeting, and *ABCD1* siRNA) were plated separately at a density of  $5 \times 10^4$  cells/well until 80–90% confluency, and then the cells were treated for 6 h with TNF $\alpha$  (10 ng/ml). Meanwhile, THP-1 cells were incubated with Calcein AM (Life Technologies; 1 mM) at a 1:1000 dilution and incubated for 1 h in the cell incubator at 37°C. The THP-1 cells were then pelleted and resuspended in RPMI Medium 1640 (Life Technologies) plus 10% foetal bovine serum and 1% penicillin-streptomycin (Life Technologies). Afterwards, the Calcein AM-labelled THP-1 cells were seeded at a density of  $1 \times 10^5$  cells/well onto the endothelial monolayer and incubated for 1 h at 37°C. Media was then removed, and each well washed with phosphate-buffered saline, and examined by fluorescent microscopy. Images were captured in four random microscopic fields at  $\times 10$  using an inverted fluorescence microscope (Nikon eclipse TE2000-U) and fluorescence was quantified using ImageJ software.

## Human monocyte transmigration assay

HBMECs were used to generate an *in vitro* model of the human blood–brain barrier, as previously described (Rubin *et al.*, 1991; Wong *et al.*, 2004). In brief, HBMECs were seeded on collagen-coated 8- $\mu\text{m}$  pore size Boyden chambers (BD Biosciences) at a density of  $5 \times 10^4$  cells per well in supplemented EBM-2 media and cultured until they formed a confluent monolayer. A suspension of  $1.5 \times 10^6$  per ml THP-1 cells labelled with Calcein AM was loaded in the upper chamber. Before transmigration assays, HBMEC and HUVEC were preactivated with TNF $\alpha$  (10 ng/ml) for 4 h.

After 2 h, the absolute number of cells that had transmigrated to the lower chamber was counted via flow cytometry.

## Statistical analysis

A multivariate two-way ANOVA with Bonferroni *post hoc* test was performed to compare immunostaining in each zone of the lesion among different disease groups and controls. Treatment effects of *ABCD1* silencing and blocking monoclonal antibodies against adhesion molecules in monocytes-endothelial cell interaction assays were analysed with one-way ANOVA followed by Tukey's test for multiple comparisons. For comparisons between two groups, Student's *t*-test was applied.  $P < 0.05$  was considered statistically significant.

## Results

### Perilesional leakage of the blood–brain barrier and perivascular inflammatory infiltration in CALD

We examined 13 human brain specimens from patients with CALD and found disruption of the blood–brain barrier at the demyelinating edge in all 13, as demonstrated by leakage of fibrinogen (an exclusively intravascular protein) into the perivascular space. We also found increased expression of MMP9 in the perilesional white matter (normal-appearing white matter as assessed by MBP stain beyond the lesion, anatomically corresponding to the U-fibres). The vast majority of MMP9 was found in microglial cells and some in astrocytes and endothelial cells. This increase in permeability and MMP9 expression extended beyond the zone of perivascular monocytic infiltration that is present at the edge of the demyelinating lesion (Eichler *et al.*, 2007). Vessels that traversed from the normal-appearing white matter into the lesion showed a consistent pattern of perivascular mononuclear cells expressing monocyte/macrophage markers (CD68) clustered at the edge of the demyelination, while activated (amoeboid-shaped) microglia (IBA1+ cells) surrounded these vessels in their entire white matter course. In contrast, microglia activation was not seen around vessels in normal appearing white matter of control and multiple sclerosis specimens (Fig. 1).

### Abnormal expression of endothelial tight junction proteins coincides with areas of blood–brain barrier breakdown

Endothelial cells of microvessels in the perilesional white matter and the core of the lesion showed displacement of both CLDN5 and ZO1 from the tight junction to the cytoplasm of endothelial cells and the perivascular space. A similar pattern was observed in the core of demyelinating multiple sclerosis lesions (Fig. 2). At the core of CALD

lesions most vessels showed some co-localization of CLDN5 and ZO1 with monocytes and microglia (CD68+ and IBA1+, respectively). Cortical white matter vessels preserved their architecture and displayed appropriate interjunctional CLDN5 and ZO1 localization. Quantification of CLDN5 and ZO1 demonstrated that these proteins were increased in the perilesional white matter, and at the core of the lesion (Supplementary Fig. 1). This increase in tight junction proteins in the perilesional white matter corresponded with an increase in the number of vessels appreciated by von Willebrand factor stain of endothelial cells. Moreover, the overall increment in the fluorescence of these proteins may represent redistribution of concentrated protein anchored in the membrane to a more diffuse and larger area in the cytoplasm as depicted in Fig. 2.

### Endothelial cells cannot compensate for the lack of ABCD1

In a first set of experiments, we investigated the capacity of ABCD1 to affect endothelial cells *in vitro*. Because of endothelial cell heterogeneity (Bastaki *et al.*, 1997; Eberhard *et al.*, 2000; Chi *et al.*, 2003), the ABCD1 dysfunction was assessed in macrovascular and microvascular endothelial cells of different origin. *ABCD1* silencing did not cause visible morphological changes in HBMECs (Supplementary Fig. 2A). After *ABCD1* siRNA, we found a reduction of >90% *ABCD1* mRNA ( $P < 0.01$ ), demonstrating successful silencing of the *ABCD1* gene. We found no increase in other ABCD family member genes (*ABCD2*, *ABCD3*, *ABCD4*) after silencing (Supplementary Fig. 2B). This may not be surprising, as several human and mouse cell types do not show compensation for the lack of ABCD1 by upregulating genes of close homology (Netik *et al.*, 1999; Muneer *et al.*, 2014). Further, within liver of the ABCD1 deficient mouse a downregulation of ABCD2 has been described (Weinhofer *et al.*, 2005). The gene expression was paralleled by a significant reduction of ABCD1 protein in *ABCD1* silenced cells, whereas no significant upregulation of other ABCD member proteins was observed in either HBMEC (Supplementary Fig. 2C) or HUVECs (Supplementary Fig. 2D).

### ABCD1-deficient brain microvascular endothelium alters tight junction proteins and adhesion molecules

The lack of compensation by other ABCD family member proteins suggests vulnerability of brain endothelium in subjects deficient in ABCD1. To evaluate the direct impact of ABCD1 deficiency upon brain endothelium, we set out to measure several key protein markers including tight junction proteins and adhesion molecules after *ABCD1* silencing. Of note, *ABCD1* silencing led to significant changes of ICAM1 and CLDN5 protein expression—around 80%

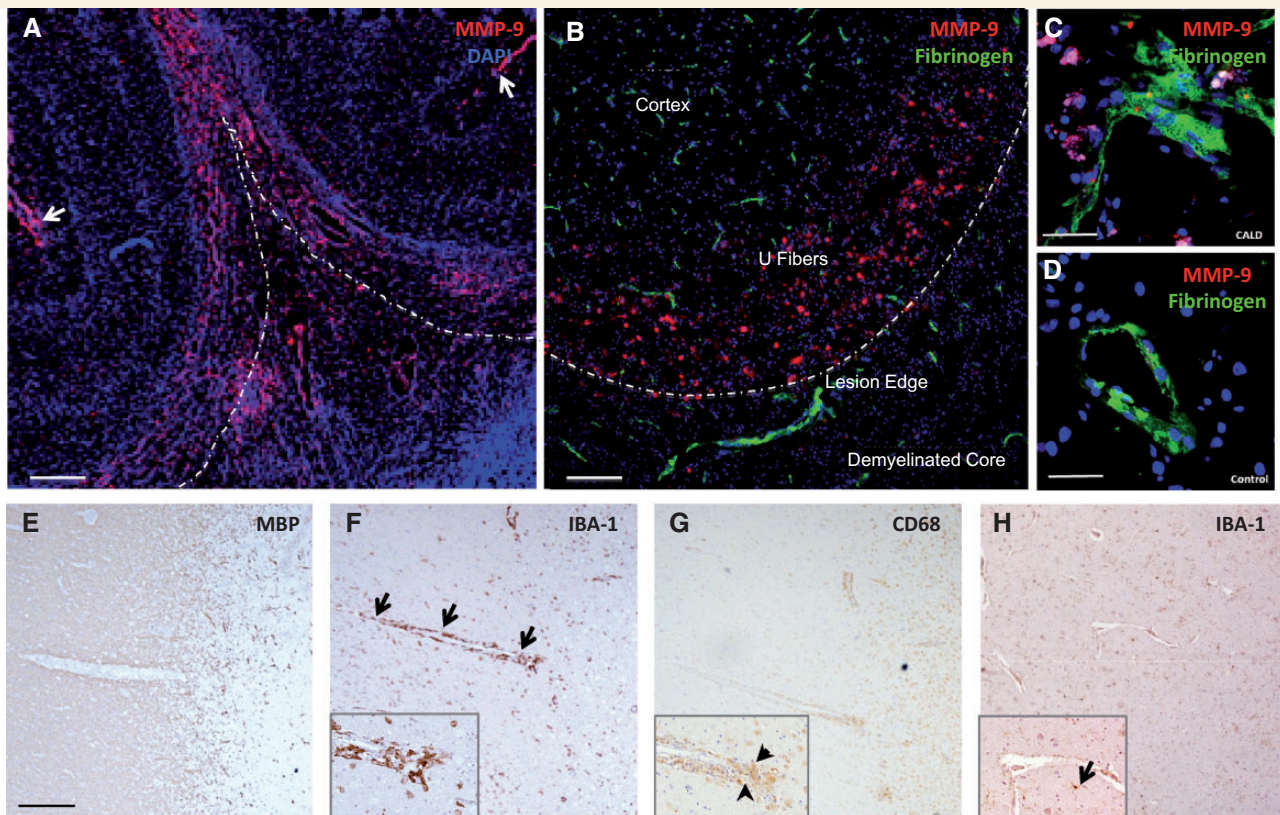


**Figure 1 Blood–brain barrier disruption in cerebral adrenoleukodystrophy.** (A) Microphotographs of brain specimen from patients with CALD shows disruption of the blood–brain barrier in perilesional white matter as evidenced by increased MMP9 expression extending beyond the inflammatory active zone at low magnification as well as (B and C) leakage of fibrinogen (an exclusively intravascular protein) into the perivascular space. Subarachnoid vessels also expressed MMP9 (arrows). (D) Control brain specimen. Anatomical regions in the upper panel are marked as cortex, U fibres, lesion edge (dashed line) and demyelinated core. Lower panel shows vessels moving from normal white matter into the demyelinated lesion apparent by the lack of myelin staining with MBP (E). Representative images show microglia (IBA1+) surrounding the entire course of the vessels (arrows) at low and high magnification (inset) in F as well as macrophages-monocytes (CD68+) clustered on the lesion end of the vessel (arrowheads) (G). This pattern of perivascular microglia activation was not observed around vessels of normal-appearing white matter of control (H) or multiple sclerosis specimens (not shown). Scale bars = 2000  $\mu\text{m}$  (A), 300  $\mu\text{m}$  (B) and 50  $\mu\text{m}$  (C and D), 500  $\mu\text{m}$  (E and H).

reduction in CLDN5 ( $P < 0.001$ ) and 70% increase in ICAM1 ( $P < 0.05$ ) (Fig. 3A and B), along with moderate reduction of ZO1 expression in HBMECs. Upon further analysis of mRNA levels, the dramatic reduction of CLDN5 mRNA expression indicated transcriptional inhibition by ABCD1 deficiency, while a lack of change in ICAM1 gene expression suggested likely post-transcriptional upregulation of ICAM1 protein (Fig. 3C,  $P < 0.01$ ). Also, the functional collapse of CLDN5 was further demonstrated by immunostaining that showed lack of CLDN5 in the intercellular space of ABCD1-silenced HBMECs. This mislocalization of CLDN5 could be devastating for the integrity of intercellular tight junctions (Fig. 3D).

To rule out potential off-target effects of the siRNA, such as the activation of the innate immune response (Robbins *et al.*, 2009) we measured TNF (TNF $\alpha$ ) mRNA levels in both control and ABCD1 siRNA treated HBMECs. We

found no increase in TNF mRNA expression after siRNA (Supplementary Fig. 3), suggesting that RNA silencing does not directly activate endothelial cell immune mediators through TNF $\alpha$ .

### TGF $\beta$ 1 increase after ABCD1 silencing

Transforming growth factor beta (TGF $\beta$ ) is known to be involved in the regulation of tight junctions. Interestingly, TGF $\beta$ 1 and TGF $\beta$ 2 mRNA exhibit alterations in opposite directions following ABCD1 silencing in HBMECs, with  $\sim 3$ -fold increase in TGF $\beta$ 1 and a non-significant decrease in TGF $\beta$ 2 mRNA (Supplementary Table 1 and Fig. 3). This suggests, as previously reported (Shimizu *et al.*, 2011; Tossetta *et al.*, 2014), that the downregulation of CLDN5 observed after silencing of ABCD1 may be mediated by increased TGF $\beta$ 1.

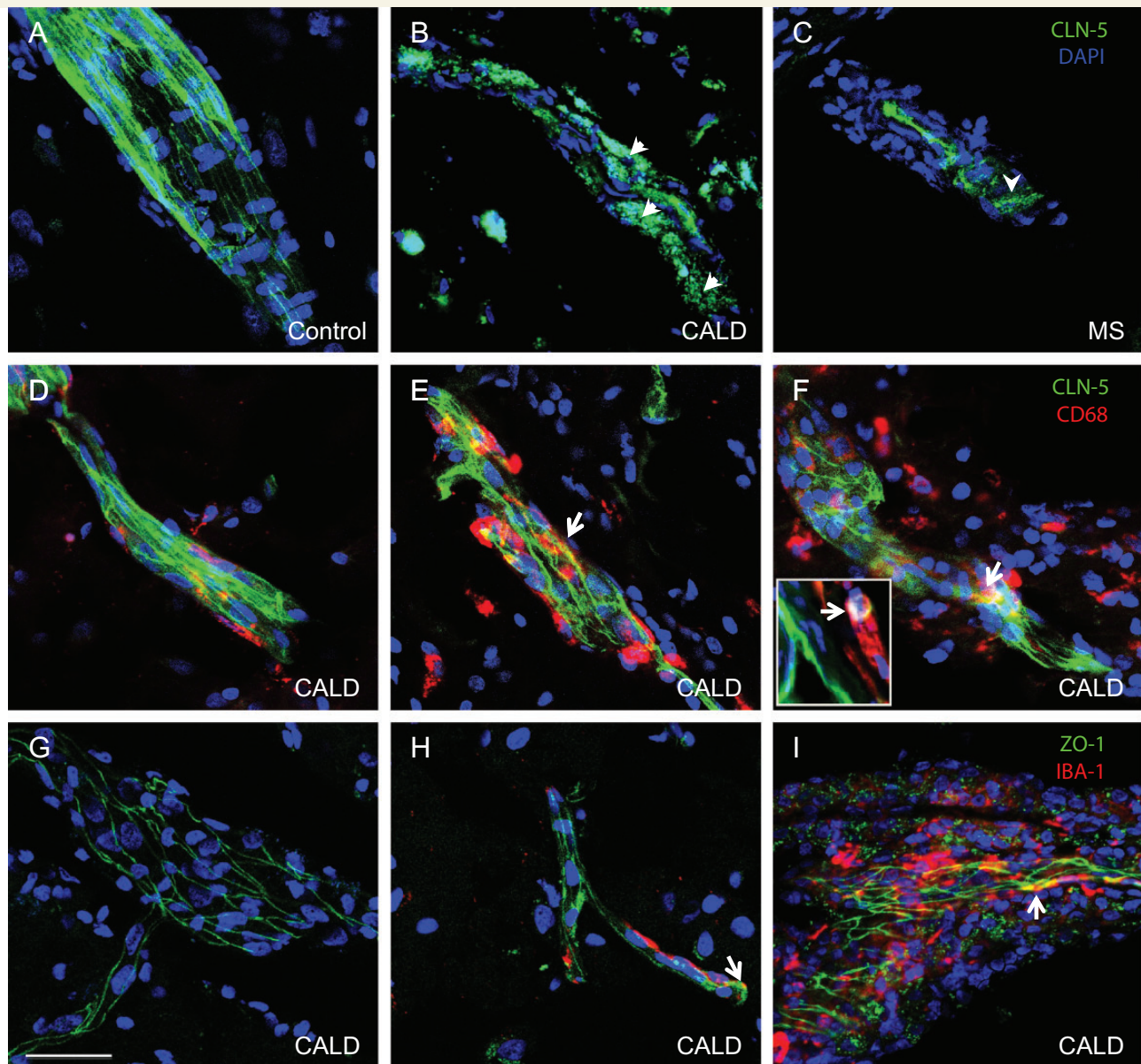


**Figure 2** Abnormal localization of CLDN5 and ZO1 expression in CALD and multiple sclerosis. Microphotographs of representative confocal imaging of CLDN5 immunostaining show intact structures of vessels and CLDN5 in the endothelial membrane in the cortex (A). Perilesional white matter vessels of CALD (B) and demyelinated plaque of multiple sclerosis brain (C) showed disrupted vascular structure and displaced CLDN5 (arrowhead) expression from tight junction to cytoplasm and perivascular space. Co-staining of CLDN5 and CD68 indicates some co-localization of CLDN5 with monocytes (CD68+) (arrows and inset) in perilesional (E) and core (F) white matter vessels but not in the cortex (D) in CALD. Co-staining of ZO1 and IBA1 indicates some colocalization of ZO1 with microglia (IBA1+) (arrows) in CALD brain (arrows) in the core of the lesion (I) but not in perilesional white matter (H) or cortical vessels (G). Scale bar = 50  $\mu$ m.

## Inflammation exacerbates ABCD1 induced endothelial protein changes

The data above indicate that ABCD1 deficiency alone is sufficient to affect endothelial protein markers. To further assess the impact of ABCD1 deficiency upon endothelium in inflammatory conditions, both HBMECs and HUVECs were silenced by ABCD1 siRNA and then exposed to TNF $\alpha$  (10 ng/ml). As shown in Supplementary Fig. 4,

HBMECs expressed higher concentrations of ABCD1, ICAM1, VCAM1 and CLDN5 than HUVECs at baseline. Upon TNF $\alpha$  stimulation, >2-fold increase of ICAM1 ( $P < 0.05$ ) and 5-fold increase of VCAM1 as well as 70% reduction ( $P < 0.01$ ) of CLDN5 were observed in HBMECs subjected to ABCD1 silencing (Fig. 4A and B). CLDN5 expression was also reduced in ABCD1 silenced HBMECs following TNF $\alpha$  treatment. This was in contrast to only 30% increase of ICAM1 and a 2-fold increase of

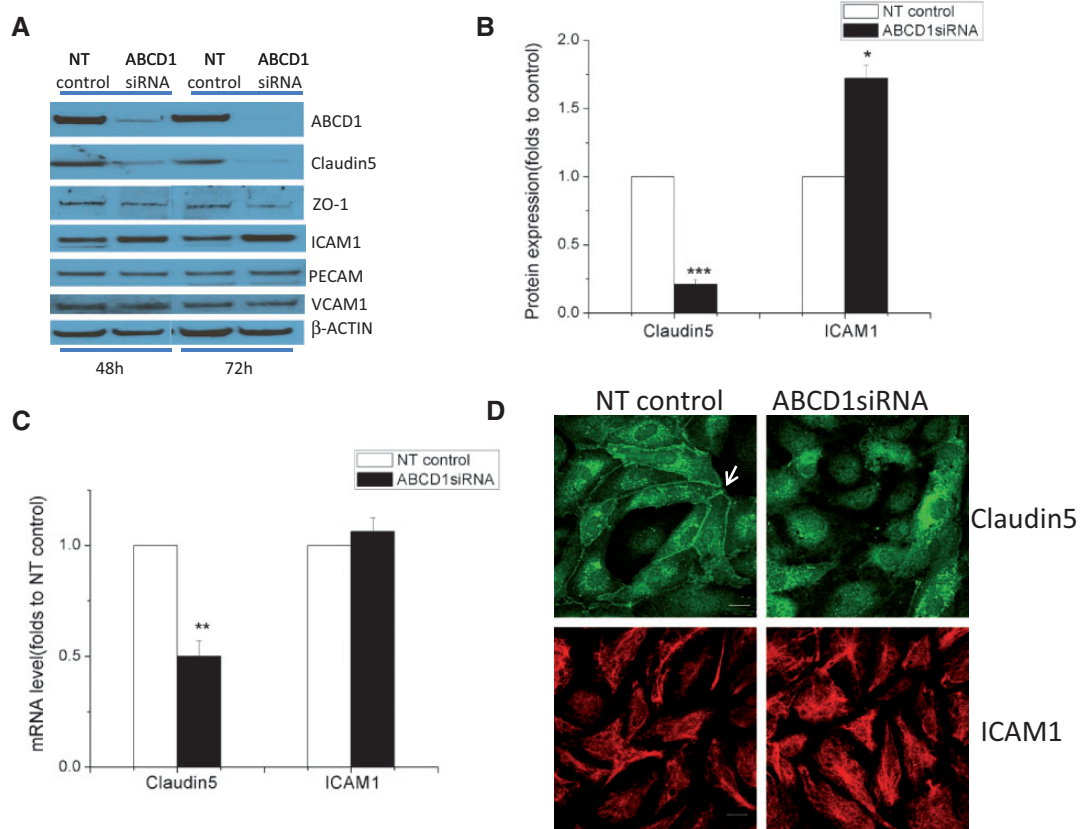


**Figure 3** Effect of *ABCD1* silencing on the expression of tight-junction proteins and adhesion molecules. (A) Changes in tight-junction proteins (CLDN5 and ZO1) and adhesion molecules (ICAM1, VCAM1 and PECAM) detected by western blot in HBMECs silenced with either non-targeting (NT) control or *ABCD1* siRNA for 48 h. Differences in CLDN5 and ICAM1 protein expression (B) and mRNA (C) quantification using ImageJ are shown as mean  $\pm$  SEM. (D) CLDN5 and ICAM1 immunofluorescence staining in HBMECs silenced with non-targeting control or *ABCD1* siRNA. White arrow indicates membrane CLDN5 staining which is diminished and displaced from the membrane in *ABCD1* siRNA treated HBMECs. Scale bar = 20  $\mu$ m. Images are representative of three different experiments where \* $P < 0.05$ , \*\* $P < 0.01$  and \*\*\* $P < 0.001$ .

VCAM1, but no CLDN5 changes, detected in HUVECs (Fig. 4C and D) suggesting higher vulnerability of brain microvasculature to *ABCD1* deficiency in the setting of inflammation.

### ABCD1 deficiency causes increased monocyte adhesion

In view of the significant molecular changes, we next set out to test the functional consequences of *ABCD1* deficiency. Although modest, significantly increased adhesion of THP-1 cells after *ABCD1* silencing was observed in HBMECs at both baseline ( $P < 0.05$ ) as well as upon TNF $\alpha$  stimulation ( $P < 0.001$ ) (Fig. 5A and C), whereas there was no change in THP-1 adhesion in macrovascular non-brain endothelial cells (HUVECs) (Fig. 5B and C). When endothelial cells were studied in flow adhesion assays under arterial, venular and capillary shear forces, HBMECs demonstrated a significant increase in both adhesion and rolling of THP-1 cells under venular and capillary

shear forces after *ABCD1* silencing compared with controls (Supplementary Fig. 5). The transmigration assay also showed an  $\sim$ 2-fold increase of THP-1 cell transmigration through the HBMEC but not the HUVEC monolayer (Fig. 5D), suggesting specificity of functional changes due to *ABCD1* deficiency in brain microvascular endothelium. Moreover, selective blockade of ICAM1 and VCAM1 with monoclonal antibodies restored the adhesion of monocytes to baseline levels (Fig. 5E,  $P < 0.001$ ), thus confirming the functional importance of ICAM1 and VCAM1 upregulation in *ABCD1*-silenced endothelium.

### Changes in endothelial function after ABCD1 silencing precede elevation of VLCFAs

As VLCFAs are widely considered a biomarker in X-ALD, and even possible surrogate of pathology, we investigated VLCFA changes following *ABCD1* silencing over time. Surprisingly, in *ABCD1*-deficient cells, the concentrations

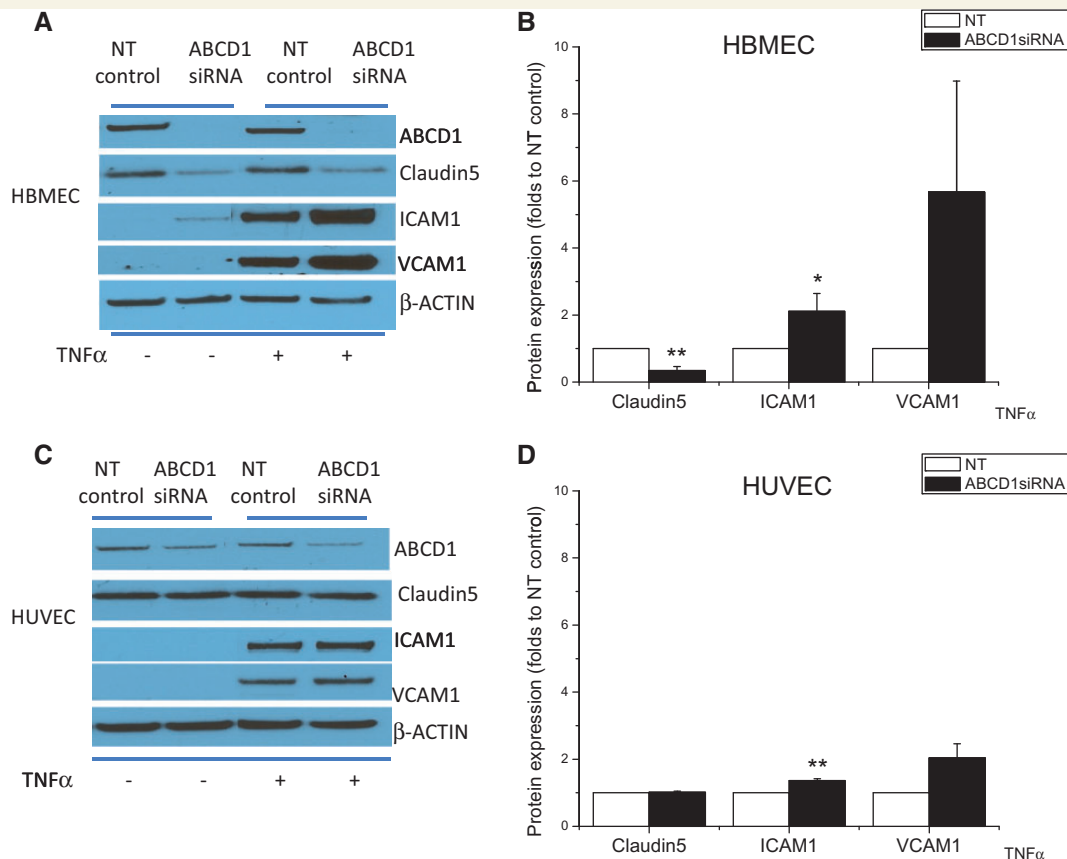


**Figure 4** Comparison of tight-junction protein and adhesion molecule expression after *ABCD1* silencing between HUVECs and HBMECs at both basal and  $TNF\alpha$ -stimulated condition. Western blot depicting ABCD1, CLDN5, ICAM1, VCAM1 in HBMECs (A) or HUVEC (C) after silencing with non-targeting (NT) control or *ABCD1* siRNA for 48 h followed by vehicle or 10 ng/ml  $TNF\alpha$  treatment for 24 h and their quantification by ImageJ (B and D). Data are mean  $\pm$  SEM of three different experiments normalized to non-targeting control and \* $P < 0.05$ , \*\* $P < 0.01$  and \*\*\* $P < 0.001$ .

of C26:0 lysophosphatidylcholine did not significantly increase until 72 h post silencing (Fig. 6A,  $P < 0.01$ ). At 48 h post-silencing, by which time massive molecular changes outlined above had occurred, C26:0 lysophosphatidylcholine was still unchanged (Fig. 6A). We next tried to assess whether exogenous VLCFAs could mimic changes in adhesion molecules and tight junction alterations seen after *ABCD1* silencing. However, high concentrations of VLCFAs produced only mild elevations of ICAM1 and yielded no changes in CLDN5 in HBMECs (Fig. 6B). In summary, *ABCD1*-silenced HBMECs altered their protein expression of ICAM1, VCAM1, CLDN5 and ZO1 >24 h before VLCFA increases, indicating an independent effect of the *ABCD1* gene on adhesion molecules and tight junction proteins.

### MYC silencing mimic the effect of *ABCD1* deficiency in HBMEC

Using a multiple sclerosis PCR-array screen, we found dramatic decreases in both mRNA and protein levels of the

transcription factor c-MYC (encoded by *MYC*) after *ABCD1* silencing in HBMECs (Fig. 7A and B,  $P < 0.001$ ). However, *ABCD1* silencing in HUVECs did not change the expression of c-MYC (Fig. 7A and B). To assess the role of c-MYC in *ABCD1*-deficient endothelial cells, we downregulated c-MYC expression in HBMECs using siRNA. Interestingly, *MYC* silencing changed the expression of CLDN5 and ICAM1 in a similar manner as *ABCD1* silencing without decreasing the levels of *ABCD1* protein itself (Fig. 7C,  $P < 0.001$ ). In parallel with protein marker changes, silencing of *MYC* also increased THP-1 adhesion to HBMEC monolayers (Fig. 7D,  $P < 0.001$ ) at both basal level and in  $TNF\alpha$ -treated conditions.

## Discussion

Our experiments demonstrate that mutant *ABCD1* in X-linked adrenoleukodystrophy (X-ALD) impacts the endothelium of brain microvasculature in ways that may be critical to initiation and progression of inflammatory demyelination. In human autopsy samples tight junction

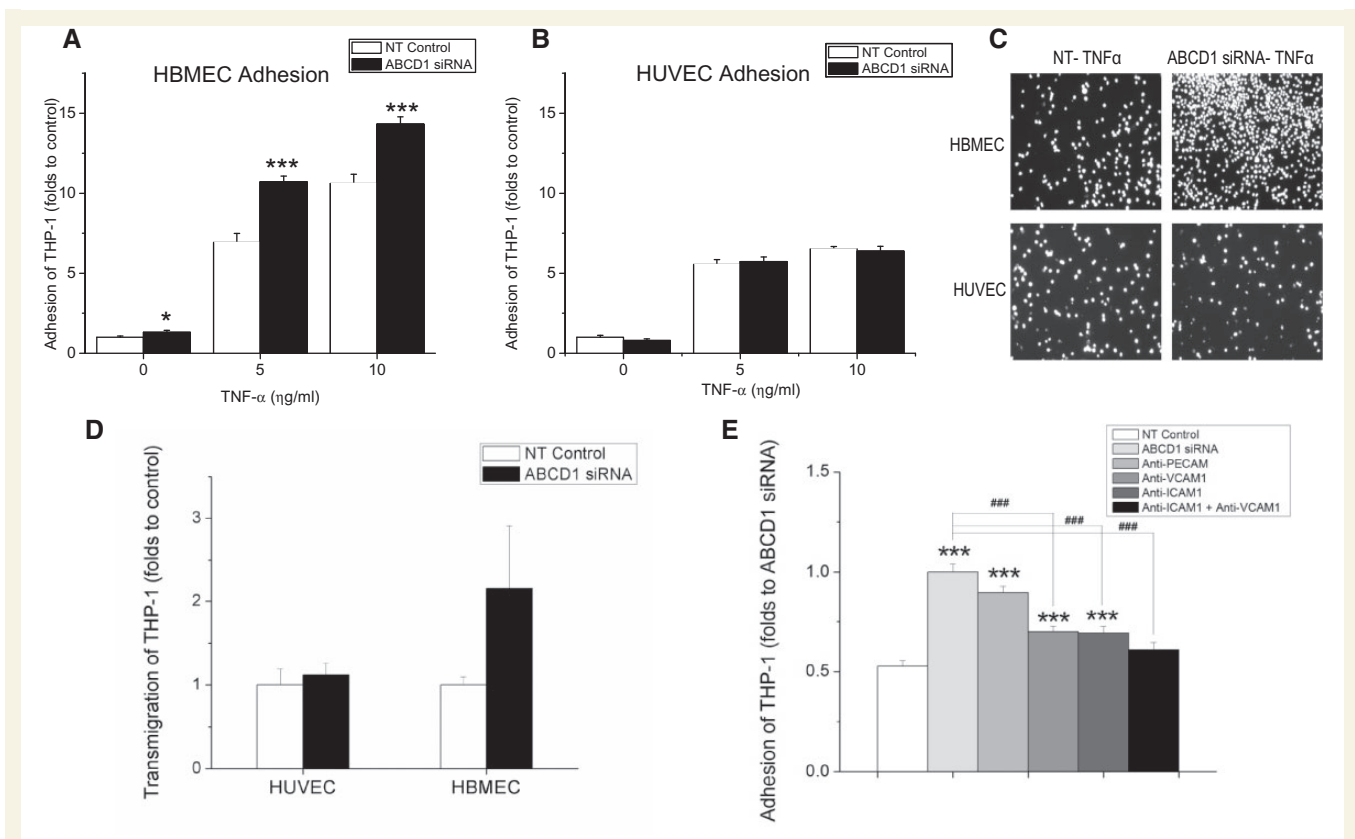


**Figure 5 Effects of *ABCD1* silencing on THP-1 adhesion and transmigration in HBMECs and HUVECs.** Adhesion of calcein AM labelled THP-1 cells to HBMECs (A) and HUVECs (B) after silencing with either non-targeting (NT) control or *ABCD1* siRNA for 48 h and treatment with 10 ng/ml TNF $\alpha$  for 4 h. (C) Microphotographs of adherent fluorescent THP-1 cells to endothelial monolayers. (D) Transmigration of THP-1 cell through activated endothelium with 10 ng/ml TNF $\alpha$  stimulation for 4 h and 2 h of 100 ng/ml MCP1 as a chemoattractant. Transmigrated THP-1 cells were measured using flow cytometry and data is shown as mean  $\pm$  SEM of two different experiments normalized to non-targeting control. (E) Effect of blocking monoclonal antibodies targeting different adhesion molecules upon adhesion of THP-1 cells to *ABCD1* siRNA silenced HBMECs compared to NT-control. Data are the mean  $\pm$  SEM of three different experiments normalized to non-targeting control. \* $P < 0.05$ , \*\*\* $P < 0.001$  as compared to non-targeting control and #### $P < 0.001$  as compared to *ABCD1* siRNA group.

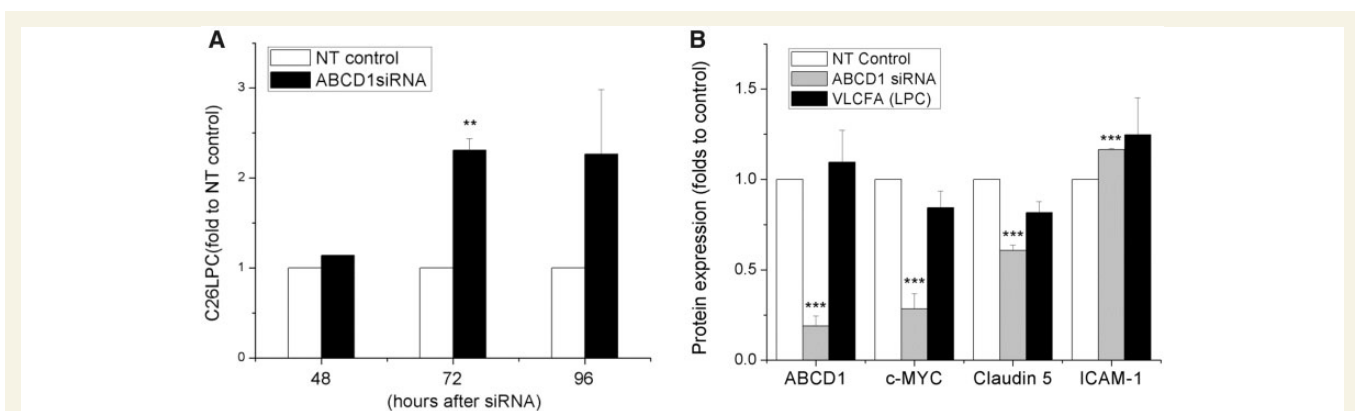


**Figure 6 VLCFA level in *ABCD1* silenced HBMECs and its effect on protein marker expression.** (A) HBMECs were silenced with non-targeting (NT) control or *ABCD1* siRNA for 48 h, 72 h and 96 h, respectively, and then cells were collected for C26:0 lysophosphatidylcholine (LPC) measurement using LC-MS. Data are mean  $\pm$  SEM of three or four different samples. \*\* $P < 0.01$ . (B) *ABCD1*, c-MYC, CLDN5 and ICAM1 protein detection by western blot in HBMECs treated with either non-targeting control, *ABCD1* siRNA or VLCFA (C26:0 lysophosphatidylcholine, 30  $\mu$ g/ml) for 48 h. Protein was quantified using ImageJ software. Data are the mean  $\pm$  SEM of three different experiments at 48 h normalized to non-targeting control and \*\*\* $P < 0.001$ .

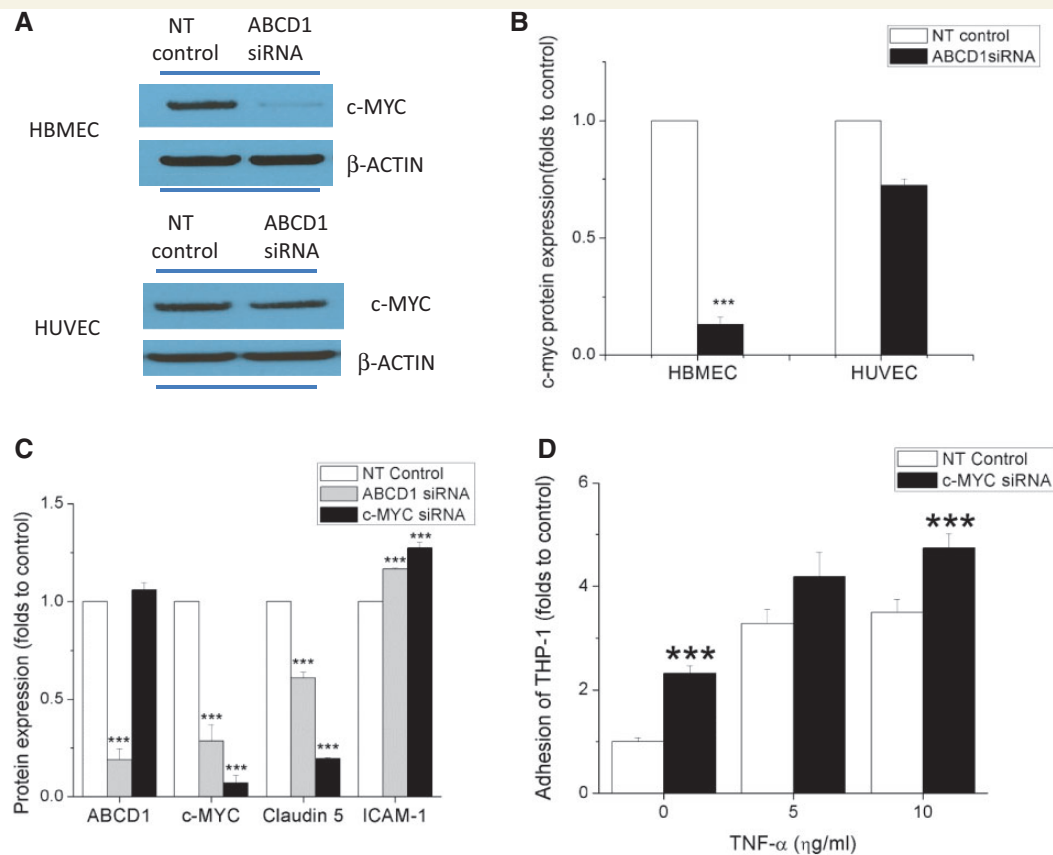


**Figure 7** *ABCD1* silencing changes protein expression and function of HBMECs through c-MYC. c-MYC expression by western blot (A) and its quantification using ImageJ (B) in HBMECs and HUVECs treated with either non-targeting (NT) control or *ABCD1* siRNA for 48 h. (C) *ABCD1*, c-MYC, CLDN5 and ICAM1 protein quantification of western blots in HBMECs following 48 h of either non-targeting control, *ABCD1* siRNA or *MYC* siRNA. (D) Adhesion of calcein AM labelled THP-1 cells to TNF $\alpha$  (10 ng/ml) activated HBMECs after silencing with *MYC* siRNA normalized to non-targeting control. Data are the mean  $\pm$  SEM of three different experiments normalized to non-targeting control and \*\*\* $P < 0.001$ .

proteins are displaced, along with massive disruption of the blood–brain barrier. When isolating brain endothelium *in vitro* RNA interference-mediated *ABCD1* gene silencing dramatically increases adhesion to monocytes and favours their transmigration. These molecular changes are further worsened by the inflammatory action of TNF $\alpha$ .

Previous observations have implicated VLCFA elevations in oxidative stress and the axonopathy seen in the *ABCD1* knockout mouse (Fourcade *et al.*, 2008; Galea *et al.*, 2012). However, the mouse model does not develop CALD, and to date no adequate model systems for CALD exist. Our data now demonstrate that *ABCD1* itself may influence brain endothelial function, and *ABCD1*-mutant HBMECs may serve as a model system to assess CALD pathogenesis and blood–brain barrier perturbation.

Several steps are required before a leucocyte can cross the blood–brain barrier and enter the brain parenchyma (Miller, 1999; Minagar and Alexander, 2003). Selectins facilitate the initial rolling and binding of leucocytes on the endothelium, whereas VCAM1, and ICAM1 facilitate endothelial adhesion of leucocytes and their

transendothelial egress. Elevation of soluble E-selectin, VCAM1 and ICAM1 has been reported in the sera and CSF of patients with multiple sclerosis, and correlates with disease activity (Droogan *et al.*, 1996).

In keeping with the observation that tight junctions are essential to the transendothelial egress of leucocytes, we demonstrate that *ABCD1* silencing downregulates cell surface expression of the tight junction proteins CLDN5 and ZO1, opening the seal that usually prevents paracellular migration. It is known that abnormalities in ZO1 and occludin occur in multiple sclerosis brains, resulting in beading or interruption of junctional integrity (Plumb *et al.*, 2002). Dysfunctional tight junctions may allow greater influx of blood-borne cells and cytokines, thus amplifying inflammation and further parenchymal damage. Both human histopathology of CALD and *in vitro* experiments showed that *ABCD1* plays an important role in the expression and distribution of CLDN5 and ZO1 and that this occurs before the elevation of VLCFA.

TGF $\beta$  is known to be involved in the regulation of endothelial barrier function and our data confirmed that *TGFB1*

mRNA and *TGFB2* exhibit alterations in opposite directions following *ABCD1* silencing (Supplementary Table 3) highlighting the complex interactions that are characteristic of signalling pathways within the TGF $\beta$  family. TGF $\beta$  exerts opposing effects on endothelial barrier function, and may be associated with increased or decreased vascular permeability depending on the downstream receptors and pathways activated (Ronaldson *et al.*, 2009). In spite of this reported dichotomy, much more is known about TGF $\beta$ 's disruptive effects on tight junctions and barrier function. Data similar to ours show increased TGF $\beta$  levels associated with decreased expression of tight junction proteins and increased permeability (Shimizu *et al.*, 2011; Tossetta *et al.*, 2014).

Evidence from both animal models and human studies support a role of MMP9 in early blood–brain barrier disruption in neuroinflammatory diseases. *In vitro* activation of brain microvascular endothelium with the proinflammatory cytokines TNF $\alpha$  and IL1 $\beta$  resulted in a selective upregulation of MMP9 expression (Harkness *et al.*, 2000). Correspondingly, some clinical studies have suggested that MMP9 is significantly elevated in patients with multiple sclerosis (Rosenberg *et al.*, 1996; Trojano *et al.*, 1999) and in the plasma and CSF of male children with CALD (Thibert *et al.*, 2012). At least one imaging study has demonstrated a correlation between MMP levels and blood–brain barrier leakage detected via contrast-enhanced MRI scans (Barr *et al.*, 2010). It is likely that the increase in MMP9 originates not only from the endothelial cells but also from the astrocytes, a major source of MMP9 and a component of the neurovascular unit (Thorns *et al.*, 2003).

Importantly, *ABCD1* showed higher levels of expression in brain microvasculature compared to the endothelium of systemic circulation. In addition to *ABCD1*, two other ABC transporters, *ABCD2* and *ABCD3*, are localized to the peroxisomal membrane (Kamijo *et al.*, 1990; Lombard-Platet *et al.*, 1996; Holzinger *et al.*, 1997). The functional unit of the *ABCD1* transporter is a dimer; *in vivo*, in the peroxisomal membrane, predominantly homodimers are formed, although heterodimers with *ABCD2* or *ABCD3*, the other two peroxisomal members of the ABCD family are possible (Berger and Gartner, 2006). Interestingly endothelial cells cannot compensate for the lack of *ABCD1* by upregulating genes of close homology as also seen in other cell types (Netik *et al.*, 1999; Muneer *et al.*, 2014; Weber *et al.*, 2014). Patients carrying the same mutation of the *ABCD1* gene can present with completely disparate phenotypes: adrenal insufficiency, adrenomyeloneuropathy and CALD. The type of *ABCD1* mutation, namely missense, nonsense, frameshift, deletion or insertion, does not predict the disease course, phenotype or response to treatment (Mosser *et al.*, 1993).

Silencing by *ABCD1* siRNA, results in late intracellular accumulation of VLCFA in human brain microvascular endothelial cells but early massive molecular reorganization, as outlined above. The increase in VLCFA following *ABCD1* siRNA silencing in HBMECs occurs around 72 h,

while endothelial function is already altered at 48 h post-silencing. Even when cells are exposed to much higher concentrations of exogenous C26:0 lysophosphatidylcholine, the effects on adhesion and tight junction proteins are minor compared with *ABCD1* silencing alone. This raises the possibility that mutant *ABCD1* causes direct endothelial cell dysfunction independent of that mediated by beta-oxidation and VLCFA accumulation.

How does endothelial dysfunction relate to human pathology? The leakage of contrast enhancement on brain MRI in patients with CALD has long suggested that dysfunction of brain vessels may be part of the pathophysiology of inflammatory demyelination in ALD (Melhem *et al.*, 2000; van der Voorn *et al.*, 2011). The extravasation of blood-borne monocytes in the perilesional white matter was further evidence of altered endothelial permeability. Alterations in endothelial function could be crucial to the pathophysiology of CALD. In our study, the large, inflammatory, demyelinating lesions reveal blood–brain barrier disruption and leucocyte transmigration into the brain, suggesting abnormal endothelium–leucocyte interactions (Fig. 3).

Relevant to this point, hematopoietic stem cell transplant (HSCT) is the only currently available modality that can arrest disease progression. While the mechanisms by which donor bone marrow-derived hematopoietic stem cells access the brain and stop demyelination are still unknown, it has been shown that they contribute to tissue vascularization during both embryonic and postnatal physiological processes (Rafii and Lyden, 2003). The length of time elapsed between engraftment and disease arrest (6–9 months) suggests that not only correction of circulating bone marrow-derived monocytes, which occurs 4–6 weeks after transplant, but also migration, hosting, and turnover of bone marrow-derived abnormal elements of the brain parenchyma is necessary. The current theory is that HSCT stabilizes function due to macrophages derived from transplanted bone marrow cells migrating into the brain and residing as microglia (Rafii and Lyden, 2003; Yamada *et al.*, 2004).

The origin of brain microglia after HSCT must be differentiated from its origin during development. Varvel *et al.* (2012) addresses the question of microglial repopulation, indicating that circulating monocytes have the potential to occupy the adult CNS myeloid niche normally inhabited by microglia in a CD11b-TK mouse model. Other research indicates that after myeloablation of bone marrow—as it is done to treat cerebral X-ALD—monocytes can give rise to macrophages but not microglia (Ajami *et al.*, 2011; Prinz *et al.*, 2011; Capotondo *et al.*, 2012). Microglial replacement *per se* originating from other sources of peripheral myeloid cells has not been fully characterized. Therefore, it is not currently known if the beneficial effect of HSCT in ALD results from microglial replacement, brain macrophage replacement or both, necessitating further study. Interestingly, we found that recruitment of IBA1+ cells (microglia) along the vessels occurs in perilesional normal-appearing white

matter indicating that microglia may play a key role in the initial demyelinating process, a phenomenon only seen in CALD and not in multiple sclerosis (Sorensen *et al.*, 1999; Trebst *et al.*, 2001; Lucchinetti *et al.*, 2011).

To date, the clinical and neuropathological manifestations of ALD have been attributed to high levels of VLCFA accumulation in white matter and peripheral nerves. Of all lipid fractions, cholesterol esters seem to have the strongest correlation with histopathology. The greatest excess of cholesterol ester levels and VLCFA enrichment is observed in actively demyelinating areas (Taketomi *et al.*, 1987; Berger *et al.*, 2014). However, even in histologically normal areas of X-ALD white matter, the phosphatidylcholine fraction contains a 39-fold excess of C26:0 compared to control, whereas the C26:0 percentage in cholesterol ester, phosphatidylserine, and phosphatidylethanolamine is either normal or increased <2-fold (Theda *et al.*, 1992).

Our results challenge the notion that demyelination in CALD is a direct consequence of VLCFA accumulation by demonstrating that changes in tight junction and adhesion molecules in brain endothelium precede the accumulation of VLCFA. Furthermore, our study found that silencing of ABCD1 also alters the expression of transcription and growth factors known to regulate blood–brain barrier permeability. It is unlikely that loss of ABCD1 function leads directly to lipid changes other than VLCFA, as this ABCD1 transporter is known to import only fatty acid-CoA, including VLCFA-CoA. On the other hand, modification of acylation of complex lipids (and proteins) can modify several signalling pathways. We cannot rule out the possibility that C26:0, in other lipids than phosphatidylcholines, or even as free fatty acids mediate metabolic processes that contribute to endothelial dysfunction. Further studies are required to assess the impact of ABCD1 downregulation on the lipid profile in endothelium and to fully elucidate the molecular mechanisms responsible for the vascular defects that follow the loss of ABCD1 activity.

Our data suggest that some of the mechanisms by which ABCD1 alters brain endothelium permeability to monocytes are mediated by c-MYC. Dramatic c-MYC downregulation occurs after *ABCD1* silencing in HBMECs alone and silencing of c-MYC mimics the protein and functional changes seen after *ABCD1* silencing. c-MYC is a transcription factor involved in cell growth, apoptosis and metabolism that has been identified as mutated in multiple human cancers and implicated in one-seventh of US cancer deaths (Dang *et al.*, 1999). In endothelium, c-MYC is essential for vasculogenesis and angiogenesis during development and tumour progression (Baudino *et al.*, 2002) and it has also been implicated in leucocyte endothelial adhesion during dissemination of lymphoma cells (Inghirami *et al.*, 1990). Downregulation of c-MYC appears to be key in mediating blood–brain barrier dysfunction and understanding its role in CALD may lead to new therapeutic targets. A preliminary network analysis of reported pathways using

MetaCore<sup>®</sup> showed that ABCD1 binds to CREB1 which binds to c-MYC and that downregulation of c-MYC causes both decreased CLDN5 and increased ICAM1. TGF $\beta$  has also a known downregulatory effect on c-MYC but no direct interaction with ABCD1 (Supplementary Fig. 6).

Although it remains challenging to establish whether vascular alterations represent the outcome of glial and/or neuronal injury, with a consequent egress of leucocytes, or are due to direct damage of endothelial cell functions, our data indicate that ABCD1 deficiency in the CNS of patients with ALD may directly affect the vascular moiety. Consequently, alterations in blood vessel integrity may contribute greatly to the CNS damage that occurs during vulnerable developmental periods of childhood. Also, our results reveal a new neuropathogenic aspect of CALD, in which the deficiency of ABCD1 activity affects the ability of the blood microvasculature to maintain barrier function in the nervous system. This may help us understand the propagation of lesions during disease evolution. Further understanding of the monocyte-endothelial interactions in ALD is critical and may affect therapeutic interventions, including bone marrow repopulation following hematopoietic stem cell transplantation (Varvel *et al.*, 2012). A better understanding of the role of the vascular system in ALD may point the way towards new endothelium-based molecular and cellular therapies (Zacchigna *et al.*, 2008).

## Acknowledgements

We thank the University of Maryland Brain and Tissue Bank.

## Funding

This study was supported by the Leblang Charitable Foundation and the National Institute of Neurological Disease and Stroke (NINDS) grants R25NS065743 and K12NS066225.

## Supplementary material

Supplementary material is available at *Brain* online.

## References

- Ajami B, Bennett JL, Krieger C, McNagny KM, Rossi FM. Infiltrating monocytes trigger EAE progression, but do not contribute to the resident microglia pool. *Nat Neurosci* 2011; 14: 1142–9.
- Barr TL, Latour LL, Lee KY, Schaeewe TJ, Luby M, Chang GS, et al. Blood-brain barrier disruption in humans is independently associated with increased matrix metalloproteinase-9. *Stroke* 2010; 41: e123–8.
- Bastaki M, Nelli EE, Dell’Era P, Rusnati M, Molinari-Tosatti MP, Parolini S, et al. Basic fibroblast growth factor-induced angiogenic phenotype in mouse endothelium. A study of aortic and microvascular endothelial cell lines. *Arterioscler Thromb Vasc Biol* 1997; 17: 454–64.

- Baudino TA, McKay C, Pendeville-Samain H, Nilsson JA, Maclean KH, White EL, et al. c-Myc is essential for vasculogenesis and angiogenesis during development and tumor progression. *Genes Dev* 2002; 16: 2530–43.
- Berger J, Forss-Petter S, Eichler FS. Pathophysiology of X-linked adrenoleukodystrophy. *Biochimie* 2014; 98: 135–42.
- Berger J, Gartner J. X-linked adrenoleukodystrophy: clinical, biochemical and pathogenetic aspects. *Biochim Biophys Acta* 2006; 1763: 1721–32.
- Berger J, Pujol A, Aubourg P, Forss-Petter S. Current and future pharmacological treatment strategies in X-linked adrenoleukodystrophy. *Brain Pathol* 2010; 20: 845–56.
- Capotondo A, Milazzo R, Politi LS, Quattrini A, Palini A, Plati T, et al. Brain conditioning is instrumental for successful microglia reconstitution following hematopoietic stem cell transplantation. *Proc Natl Acad Sci USA* 2012; 109: 15018–23.
- Chi JT, Chang HY, Haraldsen G, Jahnsen FL, Troyanskaya OG, Chang DS, et al. Endothelial cell diversity revealed by global expression profiling. *Proc Natl Acad Sci USA* 2003; 100: 10623–8.
- Cross AH, Dolich S, Raine CS. Antigen processing of myelin basic protein is required prior to recognition by T cells inducing EAE. *Cell Immunol* 1990; 129: 22–31.
- Dang CV, Resar LM, Emison E, Kim S, Li Q, Prescott JE, et al. Function of the c-Myc oncogenic transcription factor. *Exp Cell Res* 1999; 253: 63–77.
- Droogan AG, McMillan SA, Douglas JP, Hawkins SA. Serum and cerebrospinal fluid levels of soluble adhesion molecules in multiple sclerosis: predominant intrathecal release of vascular cell adhesion molecule-1. *J Neuroimmunol* 1996; 64: 185–91.
- Eberhard A, Kahlert S, Goede V, Hemmerlein B, Plate KH, Augustin HG. Heterogeneity of angiogenesis and blood vessel maturation in human tumors: implications for antiangiogenic tumor therapies. *Cancer Res* 2000; 60: 1388–93.
- Eichler F, Mahmood A, Loes D, Bezman L, Lin D, Moser HW, et al. Magnetic resonance imaging detection of lesion progression in adult patients with X-linked adrenoleukodystrophy. *Arch Neurol* 2007; 64: 659–64.
- Fourcade S, Lopez-Erauskin J, Galino J, Duval C, Naudi A, Jove M, et al. Early oxidative damage underlying neurodegeneration in X-adrenoleukodystrophy. *Hum Mol Genet* 2008; 17: 1762–73.
- Galea E, Launay N, Portero-Otin M, Ruiz M, Pamplona R, Aubourg P, et al. Oxidative stress underlying axonal degeneration in adrenoleukodystrophy: a paradigm for multifactorial neurodegenerative diseases? *Biochim Biophys Acta* 2012; 1822: 1475–88.
- Goverman J. Autoimmune T cell responses in the central nervous system. *Nat Rev Immunol* 2009; 9: 393–407.
- Harkness KA, Adamson P, Sussman JD, Davies-Jones GA, Greenwood J, Woodroffe MN. Dexamethasone regulation of matrix metalloproteinase expression in CNS vascular endothelium. *Brain* 2000; 123 (Pt 4): 698–709.
- Holzinger A, Kammerer S, Berger J, Roscher AA. cDNA cloning and mRNA expression of the human adrenoleukodystrophy related protein (ALDRP), a peroxisomal ABC transporter. *Biochem Biophys Res Commun* 1997; 239: 261–4.
- Hubbard WC, Moser AB, Liu AC, Jones RO, Steinberg SJ, Lorey F, et al. Newborn screening for X-linked adrenoleukodystrophy (X-ALD): validation of a combined liquid chromatography-tandem mass spectrometric (LC-MS/MS) method. *Mol Genet Metab* 2009; 97: 212–20.
- Inghirami G, Grignani F, Sternas L, Lombardi L, Knowles DM, Dalla-Favera R. Down-regulation of LFA-1 adhesion receptors by C-myc oncogene in human B lymphoblastoid cells. *Science* 1990; 250: 682–6.
- Kamijo K, Taketani S, Yokota S, Osumi T, Hashimoto T. The 70-kDa peroxisomal membrane protein is a member of the Mdr (P-glycoprotein)-related ATP-binding protein superfamily. *J Biol Chem* 1990; 265: 4534–40.
- Law M, Saindane AM, Ge Y, Babb JS, Johnson G, Mannon LJ, et al. Microvascular abnormality in relapsing-remitting multiple sclerosis: perfusion MR imaging findings in normal-appearing white matter. *Radiology* 2004; 231: 645–52.
- Loes DJ, Fatemi A, Melhem ER, Gupte N, Bezman L, Moser HW, et al. Analysis of MRI patterns aids prediction of progression in X-linked adrenoleukodystrophy. *Neurology* 2003; 61: 369–74.
- Lombard-Platet G, Savary S, Sarde CO, Mandel JL, Chimini G. A close relative of the adrenoleukodystrophy (ALD) gene codes for a peroxisomal protein with a specific expression pattern. *Proc Natl Acad Sci USA* 1996; 93: 1265–9.
- Lucchinetti CF, Popescu BF, Bunyan RF, Moll NM, Roemer SF, Lassmann H, et al. Inflammatory cortical demyelination in early multiple sclerosis. *N Engl J Med* 2011; 365: 2188–97.
- Man S, Ubogu EE, Williams KA, Tucky B, Callahan MK, Ransohoff RM. Human brain microvascular endothelial cells and umbilical vein endothelial cells differentially facilitate leukocyte recruitment and utilize chemokines for T cell migration. *Clin Dev Immunol* 2008; 2008: 384982.
- Melhem ER, Loes DJ, Georgiades CS, Raymond GV, Moser HW. X-linked adrenoleukodystrophy: the role of contrast-enhanced MR imaging in predicting disease progression. *AJNR Am J Neuroradiol* 2000; 21: 839–44.
- Miller DW. Immunobiology of the blood-brain barrier. *J Neurovirol* 1999; 5: 570–8.
- Minagar A, Alexander JS. Blood-brain barrier disruption in multiple sclerosis. *Mult Scler* 2003; 9: 540–9.
- Moser H, Dubey P, Fatemi A. Progress in X-linked adrenoleukodystrophy. *Curr Opin Neurol* 2004; 17: 263–9.
- Moser HW, Loes DJ, Melhem ER, Raymond GV, Bezman L, Cox CS, et al. X-Linked adrenoleukodystrophy: overview and prognosis as a function of age and brain magnetic resonance imaging abnormality. A study involving 372 patients. *Neuropediatrics* 2000; 31: 227–39.
- Mosser J, Douar AM, Sarde CO, Kioschis P, Feil R, Moser H, et al. Putative X-linked adrenoleukodystrophy gene shares unexpected homology with ABC transporters. *Nature* 1993; 361: 726–30.
- Munee Z, Wiesinger C, Voigtlander T, Werner HB, Berger J, Forss-Petter S. Abcd2 is a strong modifier of the metabolic impairments in peritoneal macrophages of ABCD1-deficient mice. *PLoS One* 2014; 9: e108655.
- Musolino PL, Rapalino O, Caruso P, Caviness VS, Eichler FS. Hypoperfusion predicts lesion progression in cerebral X-linked adrenoleukodystrophy. *Brain* 2012; 135 (Pt 9): 2676–83.
- Netik A, Forss-Petter S, Holzinger A, Molzer B, Unterrainer G, Berger J. Adrenoleukodystrophy-related protein can compensate functionally for adrenoleukodystrophy protein deficiency (X-ALD): implications for therapy. *Hum Mol Genet* 1999; 8: 907–13.
- Obermeier B, Daneman R, Ransohoff RM. Development, maintenance and disruption of the blood-brain barrier. *Nat Med* 2013; 19: 1584–96.
- Plumb J, McQuaid S, Mirakhor M, Kirk J. Abnormal endothelial tight junctions in active lesions and normal-appearing white matter in multiple sclerosis. *Brain Pathol* 2002; 12: 154–69.
- Prinz M, Priller J, Sisodia SS, Ransohoff RM. Heterogeneity of CNS myeloid cells and their roles in neurodegeneration. *Nat Neurosci* 2011; 14: 1227–35.
- Rafii S, Lyden D. Therapeutic stem and progenitor cell transplantation for organ vascularization and regeneration. *Nat Med* 2003; 9: 702–12.
- Raine CS, Cannella B, Duijvestijn AM, Cross AH. Homing to central nervous system vasculature by antigen-specific lymphocytes. II. Lymphocyte/endothelial cell adhesion during the initial stages of autoimmune demyelination. *Lab Invest* 1990; 63: 476–89.
- Raymond GV, Seidman R, Monteith TS, Kolodny E, Sathe S, Mahmood A, et al. Head trauma can initiate the onset of adrenoleukodystrophy. *J Neurol Sci* 2010; 290: 70–4.
- Robbins M, Judge A, MacLachlan I. siRNA and innate immunity. *Oligonucleotides* 2009; 19: 89–102.

- Ronaldson PT, Demarco KM, Sanchez-Covarrubias L, Solinsky CM, Davis TP. Transforming growth factor-beta signaling alters substrate permeability and tight junction protein expression at the blood-brain barrier during inflammatory pain. *J Cereb Blood Flow Metabolism* 2009; 29: 1084–98.
- Rosenberg GA, Dencoff JE, Correa N, Jr, Reiners M, Ford CC. Effect of steroids on CSF matrix metalloproteinases in multiple sclerosis: relation to blood-brain barrier injury. *Neurology* 1996; 46: 1626–32.
- Rubin LL, Hall DE, Porter S, Barbu K, Cannon C, Horner HC, et al. A cell culture model of the blood-brain barrier. *J Cell Biol* 1991; 115: 1725–35.
- Shimizu F, Sano Y, Haruki H, Kanda T. Advanced glycation end-products induce basement membrane hypertrophy in endoneurial microvessels and disrupt the blood-nerve barrier by stimulating the release of TGF-beta and vascular endothelial growth factor (VEGF) by pericytes. *Diabetologia* 2011; 54: 1517–26.
- Sorensen TL, Tani M, Jensen J, Pierce V, Lucchinetti C, Folcik VA, et al. Expression of specific chemokines and chemokine receptors in the central nervous system of multiple sclerosis patients. *J Clin Investig* 1999; 103: 807–15.
- Taketomi T, Hara A, Kitazawa N, Takada K, Nakamura H. An adult case of adrenoleukodystrophy with features of olivo-ponto-cerebellar atrophy: II. Lipid biochemical studies. *Jpn J Exp Med* 1987; 57: 59–70.
- Theda C, Moser AB, Powers JM, Moser HW. Phospholipids in X-linked adrenoleukodystrophy white matter: fatty acid abnormalities before the onset of demyelination. *J Neurol Sci* 1992; 110: 195–204.
- Thibert KA, Raymond GV, Nascene DR, Miller WP, Tolar J, Orchard PJ, et al. Cerebrospinal fluid matrix metalloproteinases are elevated in cerebral adrenoleukodystrophy and correlate with MRI severity and neurologic dysfunction. *PLoS One* 2012; 7: e50430.
- Thorns V, Walter GF, Thorns C. Expression of MMP-2, MMP-7, MMP-9, MMP-10 and MMP-11 in human astrocytic and oligodendroglial gliomas. *Anticancer Res* 2003; 23: 3937–44.
- Tossetta G, Paolinelli F, Avellini C, Salvolini E, Ciarmela P, Lorenzi T, et al. IL-1beta and TGF-beta weaken the placental barrier through destruction of tight junctions: an *in vivo* and *in vitro* study. *Placenta* 2014; 35: 509–16.
- Trebst C, Sorensen TL, Kivisakk P, Cathcart MK, Hesselgesser J, Horuk R, et al. CCR1 + /CCR5 + mononuclear phagocytes accumulate in the central nervous system of patients with multiple sclerosis. *Am J Pathol* 2001; 159: 1701–10.
- Trojano M, Avolio C, Liuzzi GM, Ruggieri M, Defazio G, Liguori M, et al. Changes of serum sICAM-1 and MMP-9 induced by rIFNbeta-1b treatment in relapsing-remitting MS. *Neurology* 1999; 53: 1402–8.
- van der Voorn JP, Pouwels PJ, Powers JM, Kamphorst W, Martin JJ, Troost D, et al. Correlating quantitative MR imaging with histopathology in X-linked adrenoleukodystrophy. *AJNR Am J Neuroradiol* 2011; 32: 481–9.
- Varvel NH, Grathwohl SA, Baumann F, Liebig C, Bosch A, Brawek B, et al. Microglial repopulation model reveals a robust homeostatic process for replacing CNS myeloid cells. *Proc Natl Acad Sci USA* 2012; 109: 18150–5.
- Weber FD, Wiesinger C, Forss-Petter S, Regelsberger G, Einwich A, Weber WH, et al. X-linked adrenoleukodystrophy: very long-chain fatty acid metabolism is severely impaired in monocytes but not in lymphocytes. *Hum Mol Genet* 2014; 23: 2542–50.
- Weinhofer I, Forss-Petter S, Kunze M, Zigman M, Berger J. X-linked adrenoleukodystrophy mice demonstrate abnormalities in cholesterol metabolism. *FEBS Lett* 2005; 579: 5512–6.
- Wekerle H, Schwab M, Linington C, Meyermann R. Antigen presentation in the peripheral nervous system: Schwann cells present endogenous myelin autoantigens to lymphocytes. *Eur J Immunol* 1986; 16: 1551–7.
- Weller M, Liedtke W, Petersen D, Opitz H, Poremba M. Very-late-onset adrenoleukodystrophy: possible precipitation of demyelination by cerebral contusion. *Neurology* 1992; 42: 367–70.
- Wilson EH, Weninger W, Hunter CA. Trafficking of immune cells in the central nervous system. *J Clin Investig* 2010; 120: 1368–79.
- Wong D, Dorovini-Zis K, Vincent SR. Cytokines, nitric oxide, and cGMP modulate the permeability of an *in vitro* model of the human blood-brain barrier. *Exp Neurol* 2004; 190: 446–55.
- Wuerfel J, Bellmann-Strobl J, Brunecker P, Aktas O, McFarland H, Villringer A, et al. Changes in cerebral perfusion precede plaque formation in multiple sclerosis: a longitudinal perfusion MRI study. *Brain* 2004; 127(Pt 1): 111–9.
- Yamada T, Ohyagi Y, Shinnoh N, Kikuchi H, Osoegawa M, Ochi H, et al. Therapeutic effects of normal cells on ABCD1 deficient cells *in vitro* and hematopoietic cell transplantation in the X-ALD mouse model. *J Neurol Sci* 2004; 218: 91–7.
- Zacchigna S, Lambrechts D, Carmeliet P. Neurovascular signalling defects in neurodegeneration. *Nat Rev Neurosci* 2008; 9: 169–81.
- Zlokovic BV. The blood-brain barrier in health and chronic neurodegenerative disorders. *Neuron* 2008; 57: 178–201.